

## Design of a High frequency Hysteresis-Controlled CMOS Buck Converter for low power Applications

<sup>1</sup> T Swapna, <sup>2</sup> M Rakesh

<sup>1,2</sup> EEE Department, SreeDattha Institute of Engineering & Science

**ABSTRACT:** This paper presents the design of a 20 MHz hysteresis-controlled CMOS buck converter using pseudo ramp techniques for ultra-low power applications. The proposed buck converter can improve the transient response using hysteresis-controlled and fixed-voltage band techniques. Using pseudo ramp technique, pseudo inductor current signal can be produced to reduce the output voltage ripple. At the same time, the sub-1-V structure leads to low power dissipation. Moreover, by adopting the inverter-based low-voltage error amplifier topology, the proposed buck converter becomes most suitable for the low-power applications. The prototype of buck converter has been designed with 180nm 2P3M CMOS technology. The operating frequency of proposed converter is 20 MHz, with an inductor of 8.5  $\mu$ H and a capacitor of 330 nF. Experimental results show that the output voltage is 0.5 V, the load current is 27 mA.

**Keywords:** Buck converter, hysteresis-controlled techniques, CMOS, pseudo ramp signal generation.

### I. INTRODUCTION

Today's electronic systems are designed with advanced manufacturing processes as there is a rapid growth in CMOS technology, in which low supply voltage is very essential. The development of CMOS technology is continued due to the need for portable applications involving low-voltage single-cell battery operations, including ADC, SRAM and filter modules are to be operated at a low supply voltage of less than 1 V. To adopt such a low-voltage environment, many literatures have been proposed [1]-[6]. These advanced VLSI systems impose new challenges on power supply design like improving stability and reliability, because the circuits are more sensitive to noise, such as overshoot and undershoot present in the supply. However, the conventional DC-DC converters with the transient response of below 100  $\mu$ s are available for 3.3/5 V applications. But, for sub-1-V applications, the quality of response should be enhanced to achieve transient response of below 10  $\mu$ s.

There are various control schemes available and hybrid control schemes are also present to design a buck converter. However, the popular fast-response of the controlled scheme involves hysteresis control. Types of hysteresis control are voltage-mode hysteresis control [7]-[9], current-mode hysteresis control [10]-[12] and digitalized hysteresis control [13]-[15]. A hysteresis current-controlled buck converter achieves high speed transient response because of the current signal transfer and also enhanced stability due to phase locked loop circuit, used to adjust the switching frequency, but the current transfer path reduces the power efficiency [12]. The digital controlling technique has a major drawback due to computational time delay coming from analog to digital conversion, algorithm computation and pulse width modulation generation in the control loop. The digital controller of [14] reduced this time delay by eliminating one switching cycle time delay.

In this paper, a voltage-mode hysteresis control scheme is proposed for fast-transient response. In the voltage-mode hysteresis controlled design, a large equivalent series resistance (ESR) of the output capacitor is used to obtain the inductor current message signal and modulate the system. The large ESR causes two effects in general, first is, it improves the accuracy by minimizing the phase delay and the second is undesired effect, leads to non-smoothness of circuit. A large output voltage ripple would affect the accuracy, even in steady state. So, a large ESR is not suitable, especially for low-voltage applications. If a small ESR is designed to reduce the output ripple, it can improve the transient period and steady state, but it may not work properly in the conventional hysteresis control. Other current sensing schemes are developed to obtain fast-transient response without requiring large ESR, but they are involved with complicated circuit. Under large ESR conditions, a more precise value of current signal can be sensed, but it would sacrifice the stability.

It is the typical concern for the proposed circuit to deal the trade-offs between ESR value and the inductor current message signal. Also, the circuit is designed for ultra low power applications, this corresponding consideration should be taken. Based on these considerations, a new hysteresis controlled buck converter is designed to tackle the issues using a pseudo ramp generator.

## II. VOLTAGE-MODE PWM CONTROL

The block diagram of voltage-mode PWM control is shown in Fig.1. The non-overlapping and driver circuit prevents the PMOS and NMOS transistors from shorting and drive them efficiently. The PMOS and NMOS transistors acts like switches. The inductor and capacitor are used to construct a filter. Whenever the PMOS transistor conducts, the current  $I_p$  of PMOS equals to the inductor current and this current increases in a certain positive slope according to the inductor value and output voltage signal. The output voltage is fed into compensator to generate the compensated signal  $V_C$ . When the ramp signal

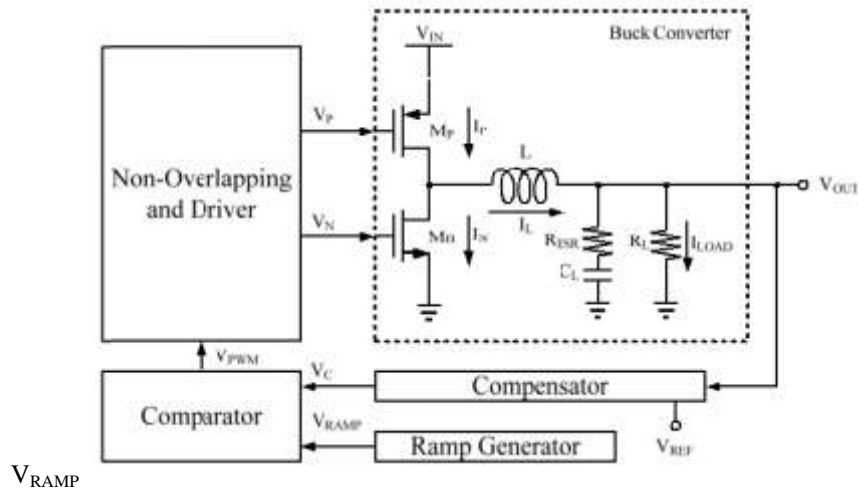


**Fig. 1.** Simplified structure of voltage-mode PWM control.

becomes higher than compensated voltage  $V_C$ , the comparator generates  $V_{PWM}$  as high. Similarly,  $V_{PWM}$  can produce both  $V_P$  and  $V_N$  signals. They can be high to turn off the high-side PMOS transistor and turning on the low-side NMOS transistor until the next clock pulse through the non-overlapping and driver.

## III. HYSTERESIS CONTROL-PSEUDO RAMP TECHNIQUE

The proposed buck converter with hysteresis control scheme using pseudo ramp technique is shown in Fig. 2. The proposed buck converter has two feedback loops. The inner loop consists of pseudo ramp generator to generate the voltage signal  $V_S$ , which resembles the inductor current signal. The outer loop passes through the compensator, fixed

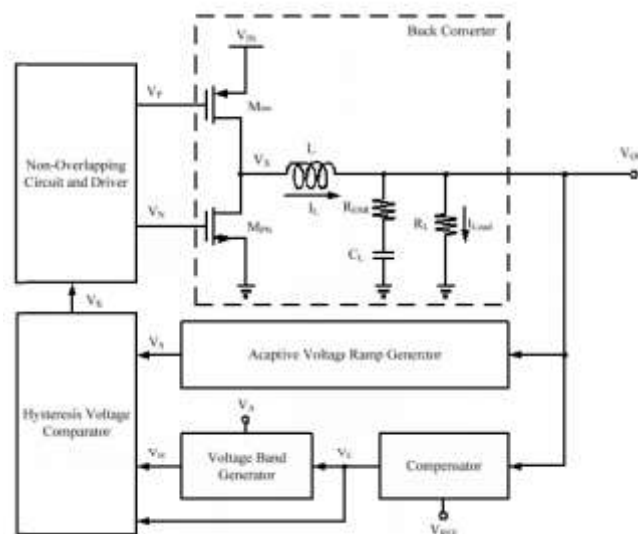


**Fig. 2.** Block diagram of proposed hysteresis-controlled buck converter using pseudo ramp technique.

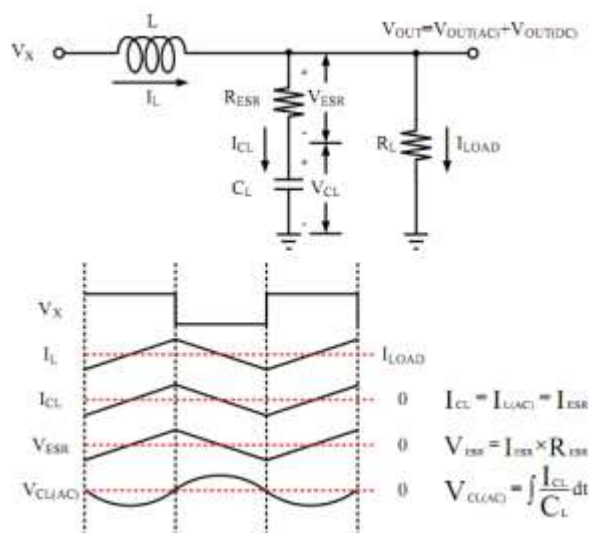


Fig. 3. Output filter of buck converter.

voltage band generator and hysteresis comparator. The output voltage is fed into the compensator with reference voltage  $V_{REF}$  to generate compensated signal  $V_C$ . The fixed band generator adds an analog voltage  $V_A$  to obtain the signal  $V_H$ . The signals  $V_H$  and  $V_C$  forms the hysteresis level and the pseudo ramp signal  $V_S$  is applied to the hysteresis comparator. Finally, the digital signal  $V_K$  is generated by the hysteresis comparator and it can be used to generate the  $V_P$  and  $V_N$  signals. The non-overlapping and driver circuit avoids the transistors from shorting and drives them efficiently.

By direct analysis, we can obtain the voltage ripple as

(1)

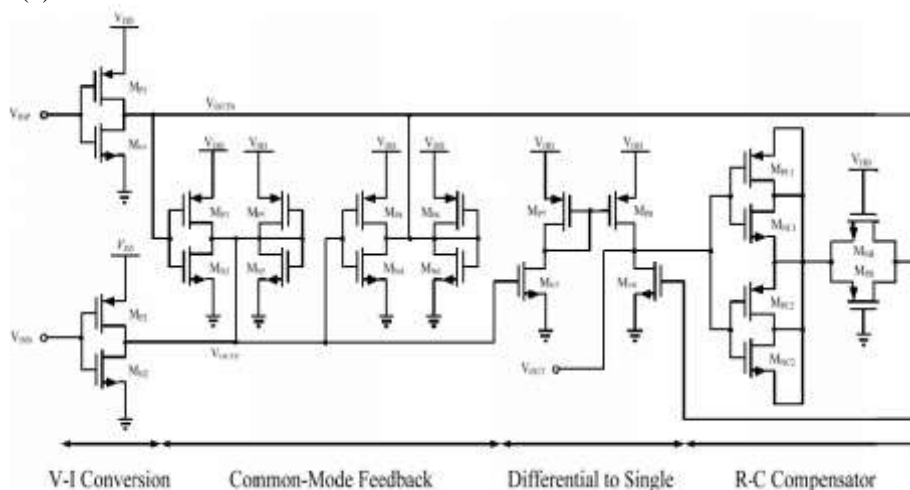


Fig. 4. Low-voltage operational error amplifier.

Based on this equation, the output ripple can be minimized by increasing the switching frequency or using a small capacitor. The output filter of the buck converter is shown in Fig. 3.  $V_{CL(AC)}$  is a part of the AC signal of the inductor current on the output capacitor. When  $V_X$  is high, the inductor current increases and  $V_{CL(AC)}$  will ramp up. When  $V_X$  is connecting to the ground, inductor current and  $V_{CL(AC)}$  will ramp down. The ESR is necessary to obtain proper inductor current sensing, but it will cause large output ripple, which affects accuracy. To overcome this problem, in this proposed converter, a pseudo ramp generator is used to produce a ramp which is similar to inductor current signal without using a large ESR of output capacitor.

**A. Pseudo Ramp Generator**

As shown in Fig. 4, the inverter-based low-voltage error amplifier consists of CMOS inverters in its V-I conversion stage[24]. The class AB operation of CMOS inverters results in low power consumption. Hence, this inverter-based low-voltage operational amplifier is most suitable to operate under 1 V with low power and high gain. The CMOS inverter has a favourable linearity when the PMOS and NMOS transistors are matched

with each other. The signal amplification is carried out by two matched inverters  $M_{P1} - M_{N1}$  and  $M_{P2} - M_{N2}$ . Additionally, the common-mode feedback (CMFB) part is composed of inverter-based latch. The group inverters  $M_{P5} - M_{N5}$  and  $M_{P6} - M_{N6}$  are diode-connected resistances between the output nodes ( $V_{OUTP}/V_{OUTN}$ ) and the common-mode voltage level. The other group inverters  $M_{P3} - M_{N3}$  and  $M_{P4} - M_{N4}$  inject the output

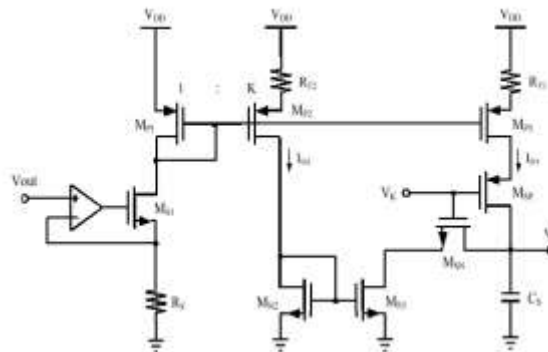
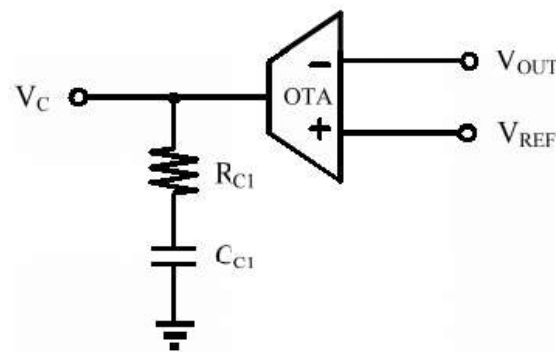
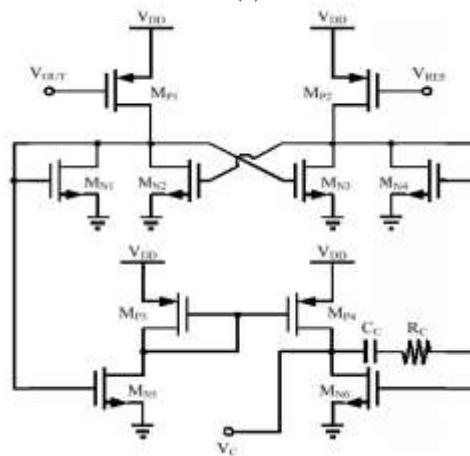


**Fig. 5.** Pseudo ramp generator.

currents into the diode-connected resistances. Thus, they become virtual loads at the output nodes. As the two group inverters having the same supply, the transconductance,  $g_m$  is equal in every group inverter. Hence, the CMFB part is operated at low-ohm load situation. The common-mode voltage level is decided by four matched inverters from  $M_{P3} - M_{N3}$  to  $M_{P6} - M_{N6}$ . In DC part, the  $M_{N,P5}$  and  $M_{N,P6}$  operates in saturation region and maintains the DC voltage at the half supply voltage to achieve the highest output swing in output differential signals. In AC part, the part of the CMFB  $M_{N,P3}$  and  $M_{N,P4}$  have gain for the amplifier. We choose  $g_{m3} = g_{m4}$ ,  $g_{m5} = g_{m6}$ , and  $g_{m3} > g_{m5}$ ; the width of the transistors of  $M_{P5} - M_{N5}$  and  $M_{P6} - M_{N6}$  are designed to be slightly smaller than those of  $M_{P3} - M_{N3}$  and  $M_{P4} - M_{N4}$ . Finally, the inverter-based low-voltage error amplifier that consists of six CMOS inverters has a large bandwidth because of the simple structure. The R-C compensation can provide the stability of amplifier with zeros and poles and the



(a)



(b)

**Fig. 6.** (a) Schematics of OTA. (b) Detail circuit.

differential-to-single circuit uses a single-stage differential amplifier with an active current mirror load. It causes the dual outputs to transfer into a single-ended output.

The pseudo ramp generator is as shown in Fig. 5. [27]. The feedback network decides the reference current  $I_S$  via  $V_{out}$  and  $R_S$  to charge or discharge the capacitor  $C_S$ . The currents of the  $I_{D1,2}$  of the pseudo ramp generator can be described as,

where  $I_S$  equals to  $V_{out}$  divided by  $R_S$ , and  $I_{D1}$  and  $I_{D2}$  equal to  $K$  times  $I_S$  when the trimming resistance equal to zero. The signal  $V_K$  is produced by comparing the signal of the pseudo ramp generator  $V_S$  with the voltage band formed by  $V_H$  and  $V_C$ . The signal  $V_K$  from the hysteresis comparator controls the operation of charging and discharging. The slope of the pseudo-inductor current signal, which is in phase with the inductor current. The equation of the pseudo-inductor current is as follows:

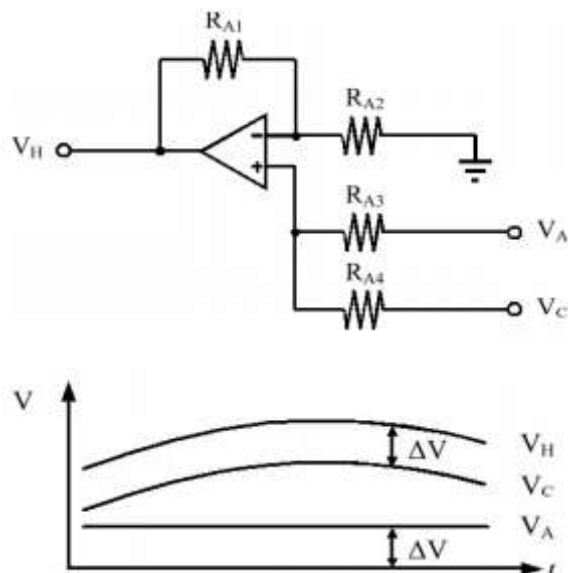


**Fig. 7.** Fixed band generator.

**B. Compensator**

Fig. 6. Shows the schematics of the operational transconductance amplifier (OTA) circuit. This circuit can generate poles and zeros to cancel the inherent poles and zeros in the buck converter. Adopting a PI compensator can generate a dominant pole and high gain at the low frequency, since the large capacitor  $C_{C1}$  at the OTA output is used to achieve the dominant pole compensation. Therefore, the large signal is very poor. After increasing  $R_{C1}$ , the zero of the compensation resistance increases the phase margin at the middle-frequency, and the large signal response of  $V_C$  becomes more elastic.

**C. Fixed Band Generator**

The fixed band generator is shown in Fig. 7. The voltage  $V_A$ , the analog voltage, which is generated by the voltage divider of  $V_{in}$ . The signal  $V_C$  adds  $V_A$  to get a precise voltage value  $V_H$  when resistors  $RA1$ ,  $RA2$ ,  $RA3$ , and  $RA4$  are identical.  $V_H$  varies with the  $V_C$  when  $V_C$  changes with the output.

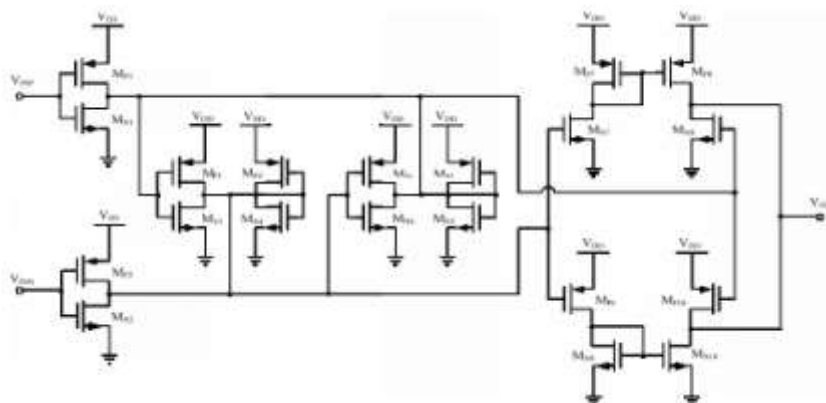


**Fig. 8.** Comparator

**D. Hysteresis Comparator**

As shown in Fig. 8, the comparator circuit is composed of digital components. The low-voltage comparator circuit has three subparts. The first part is gain amplifier circuit, which consists of two matched CMOS inverters. CMFB circuit is the second stage.

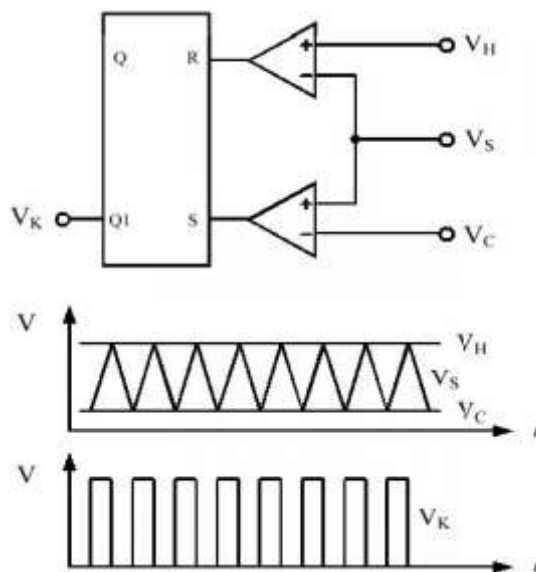


**Fig. 9.** Hysteresis comparator.

The third stage consists of two voltage-to-current converters, which are n-type and p-type. Two types of current converters decrease the input-referred offset by using a complementary structure. Finally, the digital comparator has the advantages of single-ended output and full rail-to-rail swing, wider than the conventional structures in low-voltage applications.

Fig. 9. presents the hysteresis comparator circuit with two low-voltage comparators and J-K flipflop to produce the hysteresis range with the upper limit as  $V_H$  and the lower limit as  $V_C$ . It limits the signal  $V_S$  to produce two signals into the J-K flipflop, to generate the square wave signal  $V_K$ . The hysteresis-voltage-controlled method provides the architecture to achieve fast transient responses. The switching frequency is determined by the signals  $V_H$  and  $V_C$ . When  $V_S$  is higher than  $V_H$ ,  $V_{DUTY}$  is high, and vice versa.



**Fig. 10.** Waveforms of  $V_{out}$  and  $I_L$ .

**IV. EXPERIMENTAL RESULTS**

The proposed hysteresis-controlled CMOS buck converter using pseudo ramp technique was designed with 0.18  $\mu\text{m}$  CMOS technology. The measured waveform of the output voltage, which includes  $V_{out}$  and inductor current  $I_L$ , is shown in Fig. 10, and the switching frequency is 20 MHz. Fig. 11. shows the pseudo ramp generator output  $V_S$  and inductor current  $I_L$ . As shown in Fig. 11. The signal  $V_S$  is in phase with inductor current  $I_L$ .

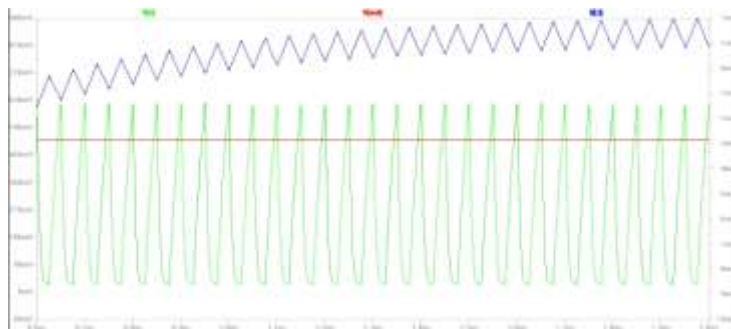


**Fig. 12.** Transient response when the load current changes with supply voltage and output voltage.



**Fig. 12.** Transient response.

**TABLE I: SUMMARY OF PERFORMANCE**

Technology	0.18 $\mu\text{m}$ 2P3M
Input voltage	1 V
Output voltage	0.5 V
Inductor	8.5 $\mu\text{H}$
Capacitor	330 nF
Operating frequency	20 MHz
Maximum Load current	2 mA
Output voltage ripple	0.00008
Transient response	
Maximum efficiency	63.5 @ 25 mA

Parameter	[8]	[28]	[29]	This paper
Technology [ $\mu\text{m}$ ]	0.35	0.13	0.5	0.18
Inductor [ $\mu\text{H}$ ]	4.7	0.00082	0.27	8.5
Capacitor [ $\mu\text{F}$ ]	10	0.02	1.6	0.33
Input [V]	3	1.2	2.7-5.5	1
Output [V]	0.5-2.5	0.4-0.96	1.2	0.5
Frequency [MHz]	0.85	90-240	20	20
Output ripple [mV]	N.A.	25	4	
Maximal load current [mA]	500	240	600	320
Maximal efficiency [%]	94.5 @ N.A.	80 @ 200 mA	84.5 @ 250 mA	

The measured performance summary of the proposed buck converter is given in Table I. In this design, the supply voltage is 1 V. In Table II, the proposed converter is compared with the state-of-the-art circuits [8], [28], [29]. In [8], the switching frequency is approximately 850 kHz, and off-chip inductor and output capacitor are 10  $\mu\text{H}$  and 4.7  $\mu\text{F}$ , respectively.

## V. CONCLUSION

The proposed 20 MHz hysteresis-controlled CMOS buck converter using pseudo ramp techniques is designed with 0.18- $\mu\text{m}$  2P3M CMOS processes. The pseudo ramp generator effectively solves the large output ripple problem with large ESR capacitor. The proposed buck converter demonstrates an extremely fast transient response and high efficiency at 1-V supply voltage. Compared with conventional buck converters, this design has the major advantages, including fast response, low number of components, low power supplies, and simple circuit structure for design and implementation.

## REFERENCES

- [1]. Y.S.Hwang, M.S.Lin, B.H.Hwang, and J.J.Chen, "A 0.35  $\mu\text{m}$  CMOS sub-1 V low-quiescent-current low-dropout regulator," in *Proc. Asian Solid-State Circuits Conf.*, Nov. 2008, pp. 153–156.
- [2]. C.Y.Leung, P. K.T. Mok, and K.N.Leung, "A 1 V integrated current-mode boost converter in standard 3.3/5 V CMOS technologies," *IEEE J.Solid-State Circuits*, vol. 40, no. 11, pp. 2265–2274, Nov. 2005.
- [3]. T. Fuse, M. Ohta, M. Tokumasu, and H. Fujii, "A 0.5 V power-supply scheme for low-power system LSIs using multi-V<sub>th</sub> SOI CMOS technology," *IEEE J.Solid-State Circuits*, vol. 38, no. 2, pp. 303–310, Feb. 2003.
- [4]. M.H.Huang, Y.N.Tsai, Y.H.Lee, S.J.Wang, K.H.Chen, Y.H.Lin, and G.K.Ma, "Sub-1 V input single-inductor dual-output (SIDO) DC-DC converter with adaptive load-tracking control (ALTC) for single-cell-powered system," in *Proc. ESSCIRC Conf.*, Sep. 2009, pp. 268–271.
- [5]. H. W. Huang, K. H. Chen, and S. Y. Kuo, "Dithering skip modulation, width and deadtime controllers in highly efficient DC-DC converters for system-on-chip applications," *IEEE J.Solid-State Circuits*, vol. 42, no. 11, pp. 2451–2465, Nov. 2007.
- [6]. C.Y.Leung, P.K.T.Mok, K.N.Leung, and M.Chan, "An integrated CMOS current-sensing circuit for low-voltage current-mode buck regulator," *IEEE Trans. Circuits Syst. II, Exp. Briefs*, vol. 52, no. 7, pp. 394–397, Jul. 2005.
- [7]. M.Siu, P.K.T.Mok, K.N.Leung, Y.H.Lam, and W.H.Ki, "A voltage-mode PWM buck regulator with end-point prediction," *IEEE Trans. Circuits Syst. II, Exp. Briefs*, vol. 53, no. 4, pp. 294–298, Apr. 2006.
- [8]. F.Su, W.H.Ki, and C.T.Tsui, "Ultrafast fixed-frequency hysteretic buck converter with maximum charging current control and adaptive delay compensation for DVS application," *IEEE J.Solid-State Circuits*, vol. 43, no. 4, pp. 815–822, Apr. 2008.
- [9]. M.Castilla, L.G.D. Viccnu, J.M.Guerrero, J.Matas, and J.Miret, "Design of voltage-mode hysteretic controllers for synchronous buck converters supplying micro processor loads," *IEE Proc. Electric Power Appl.*, vol. 152, no. 5, pp. 1171–1178, Sep. 2005.
- [10]. K.H.Chen, C.J.Chang, and T.H.Liu, "Bidirectional current-mode capacitor multipliers for on-chip compensation," *IEEE Trans. Power Electron.*, vol. 23, no. 1, pp. 180–188, Jan. 2008.
- [11]. Z.Yao, L. Xiao, and Y.Yan, "Dual-buck full-bridge inverter with hysteresis current control," *IEEE Trans. Ind. Electron.*, vol. 56, no. 8, pp. 3153–3160, Aug. 2009.
- [12]. J.J.Chen, "A nonactive current-sensing constant-frequency HCC buck converter using phase-frequency-locked techniques," *IEEE Trans. Ultra-son., Ferroelectr., Freq. Control*, vol. 55, no. 4, pp. 761–769, Apr. 2008.